SOLAR SYSTEM AND SPACE ENVIRONMENT

https://doi.org/10.18524/1810-4215.2024.37.315007

USING SYNTHETIC LIGHT CURVES OF ARTIFICIAL SATELLITE MODEL TO TEST THE PATTERNS METHOD FOR DETERMINING THE ROTATION AXIS ORIENTATION

N.I.Koshkin[1], L.S.Shakun[1], E.A.Korobeynikova[1], S.M.Melikyants[1], S.L.Strakhova[1], O.M.Kozhukhov[2]

[1] Astronomical Observatory of Odesa I. I. Mechnikov National University, 1v Marazliivska St, Odesa, Ukraine

[2] National Space Facilities Control and Test Center of the State Space Agency of Ukraine, Kyiv, Ukraine

ABSTRACT. In this paper we test a new method for determining the rotation axis direction in space for various resident space objects (RSOs). This method (Koshkin et al., 2024) is based on the structural analysis of the light curves of such RSOs and the search for similar fragments, called "photometric patterns", in observations obtained from one or several observatories simultaneously or over a short period of time. The method does not require prior knowledge of the RSO shape and does not impose strict requirements on the quality of observations, and this is its main advantage. First of all, this method is certainly applicable to rapidly rotating objects of complex shape with smooth surfaces. As a result, such RSOs are capable to reflect sunlight in a specular manner, when short-term brightness flares are present in the light curves forming a unique pattern. Identical patterns are observed when the angle between the phase angle bisector (PAB) and the rotation axis reaches the same values. However, the light curves of many RSOs have a significant diffuse component in addition to the specular flares. This diffuse component depends on both the phase angle value and the orientation of the phase angle plane relative to the RSO's plane of rotation. This paper is devoted to checking the assumption that the structure and shape of diffuse-specular patterns will remain similar to themselves within certain limits of variation of the value of these two angles at moments of equality of the PABs' latitude. The analysis is based on simulation using synthetic light curves of the RSO model, observed from several points on the Earth's surface.

Keywords: space object, model, light curve, photometric pattern, rotation axis.

АНОТАЦІЯ. Знання кінематичних властивостей, таких як кутова швидкість обертання та просторове положення осі обертання, великих відпрацьованих супутників і корпусів ракет, необхідна для прогнозування їхньої орієнтації в кожний момент часу. Ця інформація має вирішальне значення як, наприклад, для успіху місій активного видалення з орбіти цих об'єктів, так і для підвищення точності прогнозування їх орбітального руху на низьких навколоземних орбітах. Визначення стану обертання штучних космічних об'єктів (КО) здійснюється різними засобами, проте історично це робилося за допомогою оптичних наземних датчиків (фотометрів) шляхом отримання кривих блиску, їх обробки та аналізу. У цій роботі ми тестуємо новий метод для визначення напрямку осі обертання у просторі резидентних космічних об'єктів. Цей метод заснований на структурному аналізі кривих блиску таких об'єктів та пошуку схожих фрагментів ("фотометричних патернів"), у спостереженнях, які отримані з однієї або кількох обсерваторій одночасно або протягом короткого періоду часу. Основна перевага даного методу полягає в тому, що його використання не вимагає знання форми КО і не висуває жорстких вимог до якості спостережень. Перш за все, цей метод безумовно застосовується до складних за формою об'єктів, що швидко обертаються, мають у складі гладкі поверхні і, внаслідок цього, здатні відбивати сонячне світло дзеркально, в результаті чого в кривих блиску присутні короткочасні спалахи блиску утворюють унікальний патерн. Однакові патерни спостерігаються тоді, коли кут між бісектрисою фазового кута і віссю обертання досягає тих самих значень. Однак, крім дзеркальної складової, криві блиску багатьох КО мають значну дифузну складову, яка залежить як від величини фазового кута, так і від орієнтації площини фазового кута щодо площини обертання. Дана робота присвячена перевірці того припущення, що структура і форма дифузно-дзеркальних патернів залишатиметься подібною в деяких межах варіації величини цих двох кутів у моменти коли широти бісектрис бувають однаковими. Аналіз зроблено на основі синтетичних кривих блиску моделі КО, спостереження якої імітуються з декількох пунктів на поверхні Землі.

Ключові слова: космічний об'єкт, модель, крива блиску, фотометричний патерн, вісь обертання.

1. Introduction

Knowledge of kinematic properties, such as angular velocity of rotation and spatial position of the rotation axis, for large defunct satellites and upper stages of launch vehicles is necessary to predict their orientation at any given

time. This information is of crucial importance, for example, for the success of active debris removing (ADR) missions for these objects, as well as for improving the accuracy of predicting the orbital motion of space objects at LEO. The rotation state of artificial space objects (SOs) is determined by various means, but historically it has been done using optical ground-based sensors (photometers) by obtaining light curves, processing and analyzing them. The period of proper rotation of a SO around its center of mass can be fairly easily estimated by measuring the period of brightness variations. However, determining the SO's rotation axis direction in space is much more difficult if the shape of this SO is often insufficiently known. Most studies on this topic offer specific methods for determining the SO's rotation axis orientation, that are suitable only for a certain type of objects.

The attempt to solve the general problem of the so-called "inversion" of the light curve, as well as attempts to separate the contribution of the SO shape and the orientation of its rotation axis to the external view of light curves, have not been successful even for fairly simple non-convex bodies. Nevertheless, one of the real ways to perform the inversion of light curves (or determination the SO's shape and rotation axis orientation) is, first of all, the ability to estimate the current direction of the rotation axis in space. Therefore, the development of new approaches to determining the rotation axis orientation, in particular, based on photometry, remains actual.

In this paper, we use and test a new method for estimating the SO rotation axis direction in space. This method is based on the structural analysis of SO light curves and the search for similar fragments, which we call "photometric patterns", in observations obtained from one or several observatories (or observation points, OPs) simultaneously or over a short period of time (Koshkin et al., 2024). The main advantage of this method is that its use does not require knowledge of the SO shape. In addition, this method does not require a very high frequency of brightness measurements and high accuracy of the timing of photometric observations, i.e., in fact, it does not put forward strict requirements for the quality of observations. Nevertheless, it also has its constraints. First of all, this method is certainly applicable to objects with complex shapes that have smooth surfaces and, as a result, are capable of reflecting sunlight in a specular manner. In the structure of the light curves of such SOs, one can expect the presence of short-term brightness flares. If several such "specular" flares were observed in the light curve during one rotation of the SO, they can form a unique photometric pattern (in the sense of unique intervals between the specular flares). A similar pattern can also be observed in another light curve, for example, obtained at another observatory or during another passage of the given SO. In this case, it can be stated that the same patterns are observed when the angle between the PAB and the rotation axis reaches equal values in both cases (Fig. 1). However, in addition to the specular component, the light curves often have a significant diffuse component depends both on the phase angle value and on the orientation of the phase angle plane (light scattering plane) relative to the rotation plane (θ angle in Fig. 1). We assume that within certain limits of variation of these two geometric factors, the structure and shape of diffuse-specular patterns will remain similar to themselves, provided that the latitudes βi of these PABs are equal at the moments of observation of these patterns. This paper is devoted to check this assumption based on input data in the form of simulated synthetic light curves of the SO model observed from several sites on the Earth's surface.

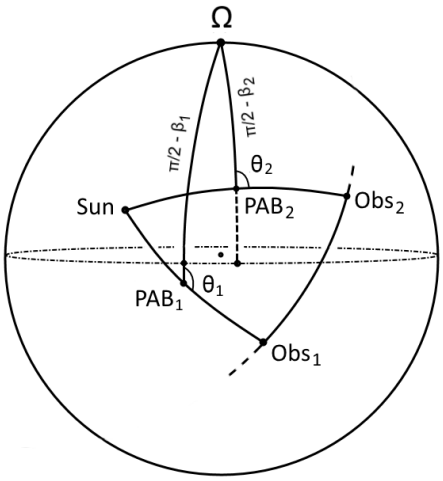

Figure 1: Satellite-centric position of the main vectors that determine the conditions of its illumination and visibility. Arc "Sun-Obs$_i$" determines the current phase angle. Arc "Ω-PAB$_i$" is equal ($\pi/2 - \beta_i$), where β_i – PAB latitude relative to the pole of the rotation axis Ω. Angle θ_i determines the current position of the light scattering plane relative to the SO's rotation plane.

2. Simulation technique

In the method of photometric patterns (Koshkin et al., 2024), to find the RSO rotation axis orientation, it is necessary to obtain photometric observations from one or several OPs in a quantity sufficient to identify several types of patterns on the light curves (each pattern needs to be detected at least twice) over a sufficiently short time interval (the desired RSO rotation axis orientation can be considered fixed during this interval).

In order to be sure to detect the same photometric pattern on different light curves of a given SO, it is necessary that the mutual configurations of the three vectors mentioned above (the rotation axis and the satellite-centric directions to the Sun and to the observer) were identical. On the other hand, to determine the rotation axis direction, we need the directions of the PAB vectors in the inertial space for the same photometric pattern have to be maximally different. This contradiction can be overcome if the photometric pattern can be reproduced with different configurations of the said vectors. It is always true for "specular" patterns and, as we will show below, it is also possible for "diffuse-specular" patterns.

In practice, we currently do not have a sufficient number of observations of any RSO obtained in the required geometry, and it limits the possibility of making reliable estimates of the direction of the RSO rotation axis in the inertial coordinate system. However, it is possible to use synthetic light curves of the RSO model obtained using animation and visualization programs for three-dimensional scenes such as Blender (Kudak et al., 2024), 3D-Max (https://

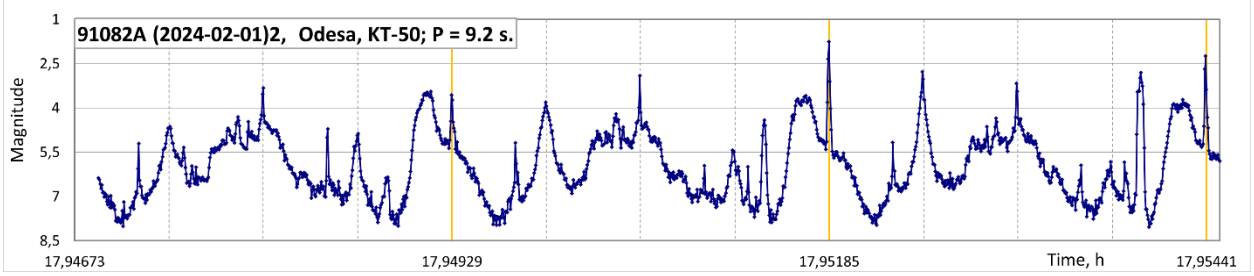

Figure 2: A fragment of the light curve of the spacecraft 91082A (DMSP 5D-2 F11), obtained on February 1, 2024 in Odessa on the KT-50 telescope in tracking mode. The rotation period of the spacecraft is 9.2 seconds (it is marked with vertical lines on the light curve).

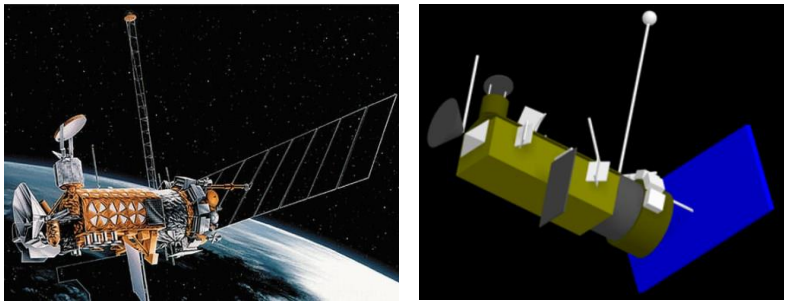

Figure 3: The spacecraft DMSP 5D3 and model used to calculate the synthetic light curves

Table 1: Optical characteristics of the spacecraft model's individual parts specified in 3D-Max

Nomenclature	Color (RGB)	Diffuse Color	Specular Level	Glossiness
Main body of model	80, 80, 0	80, 80, 0	15	90
Small boxes, Small panels, Rods	150, 150, 150	150, 150, 150	990	100
Cylinder, cone, screen, disk	50, 50, 50	50, 50, 50	100	100
Solar Panel	0, 0, 170	0, 0, 170	10	60

help.autodesk.com/view/3DSMAX/2023/ENU/), etc. We have accumulated experience using the 3D-Max package (Koshkin et al., 2018; 2019), which allows us to generate a fairly adequate geometric shape of the RSO model using the Max-script language, to set the required coefficients of diffuse and specular reflection of light for each elementary surface, as well as its color.

It is also important that in any simulator it is possible to set the correct ratio of the distances between the light source, the model and the radiation receiver in relation to the model dimensions. Since the observer always sees the RSO as a point source of light illuminated by the Sun's rays, all rays reflected towards the observer in a narrow solid angle (almost parallel to each other), for example, from all areas of a large flat surface of solar panels, should simultaneously hit the receiver. Otherwise, if the distance to the model is comparable to its dimensions, such a panel will be "visible" to the receiver in parts, i.e. "scanning" will be observed and a light flare, for example, from two strictly parallel solar panels located on both sides of the satellite body will look like a double one, which is not observed for real RSOs in orbit.

We used the 3D-Max package and a model whose shape is approximately similar to a DMSP-type spacecraft (https://space.skyrocket.de/doc_sdat/dmsp-5d2.htm) for our task. There are many observations of objects of this series in our photometric database (Koshkin et al., 2017; 2021), and it can be noted that many of them often demonstrate periodicity of light changes, have a complex structure of light curves and the presence of a significant number of specular flares. As an example, Fig. 2 shows a fragment of the light curve of the spacecraft with COSPAR ID 91082A (DMSP 5D-2 F11). Fig. 3 shows an images of the spacecraft and model used to obtain synthetic light curves. Table 1 contains the optical parameters that we used to specify the optical properties of light reflection for different surfaces of this model.

It was assumed the model rotates stably around a fixed axis, rigidly connected to the body, which is perpendicular to the base and longitudinal axis of the satellite. In this case, we have a flat rotation of the model around one axis, which also maintains its orientation in inertial space over relatively short time intervals.

3. Results of light curves simulation for different observation points

Simulations of the synthetic light curves of the model were made for several OPs located in different places in the northern and southern hemispheres (see Table 2).

To calculate the visibility conditions of the model from different locations, a real near-Earth orbit similar to the orbit of the 22154B spacecraft (i = 98.75, e = 0014, n = 14.17) and typical conditions of object observability were used. To model the light curves, the date of 02.12.2024 was selected, when visibility was realized from all seven selected OPs. We considered only those passages of SO when the trajectories of the PAB vectors fall into a common region (see Fig. 4a)) and, accordingly, the PAB latitudes can have a common range of change. For this purpose, in subsequent calculations of the light curves, the pole of the model rotation axis, was taken in the direction determined by the equatorial coordinates ($\alpha\,\Omega = 260°$, $\delta\,\Omega = +23°$). The graphs of the change in the PAB latitude over time in the coordinate system associated with this rotation axis for all selected passages are shown in Fig. 4b). We can see that the ranges of latitude change PAB overlap well in groups separately for northern and southern observation points. For the selected pole of rotation, these groups also partially overlap each other in the latitude range of about +24° ÷ +38°.

Let us now consider the obtained synthetic light curves of this model for the given observation conditions. The rotation period of the model was 18 sec and up to 30 complete rotations were observed in different passes. Therefore, it is possible to present all the light curves in their entirety only on a very compressed scale. We will present here only 5-6 fragments of each light curve, which most fully reflect the change in their shape over time. Figures 5a) and 5b) show sequential fragments of the light curves for three northern and four southern OPs.

Table 2: Observation points locations used for simulation of the synthetic light curves

Site Name	Abbreviated Name	Geographical latitude, deg	Geographical longitude, deg
Odesa	Ods	46.5	30.7
Novosilki	Nov	50.6	30.6
Lviv	Lvi	49.9	24.0
New Zealand	NZel	–44.0	170.5
Northern Australia	NAus	–17.6	123.8
South Africa	SAfr	–32.4	20.7
Argentina	Arg	–45.6	–69.1

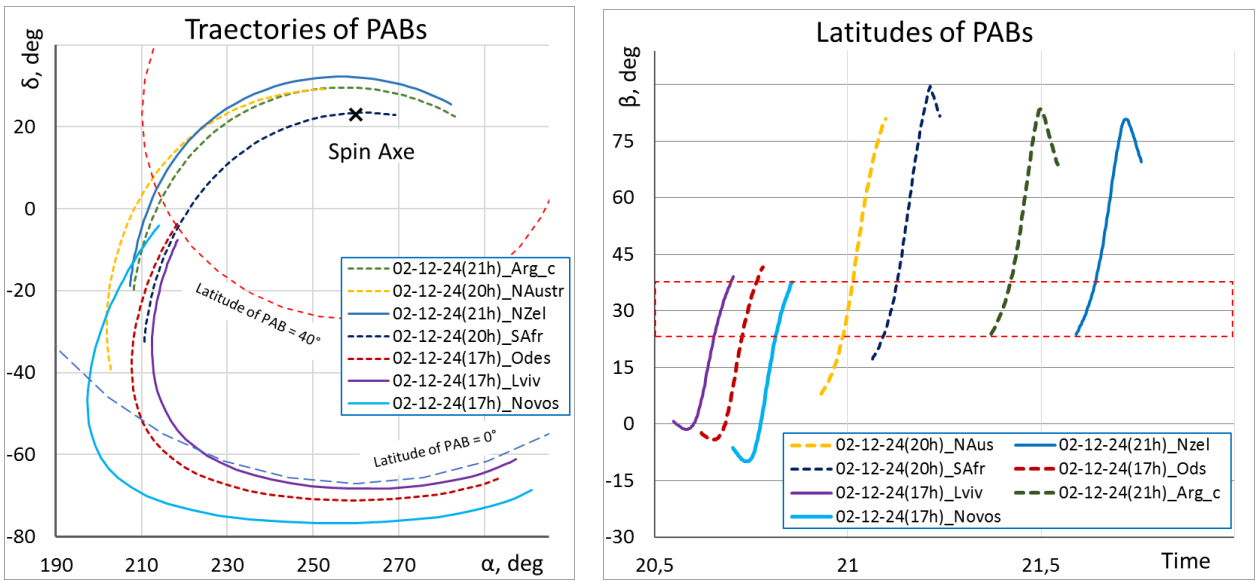

Figure 4: a) – Trajectories of PAB vectors in seven passes of the SO model over different OPs, for which synthetic light curves were calculated. The cross indicates the selected pole of the model's rotation axis, for which two latitude circles are shown. b) – Graphs of the change in latitude of PAB over time for these passages with the selected position of the pole of the rotation axis (graphs are arbitrarily shifted along the time axis).

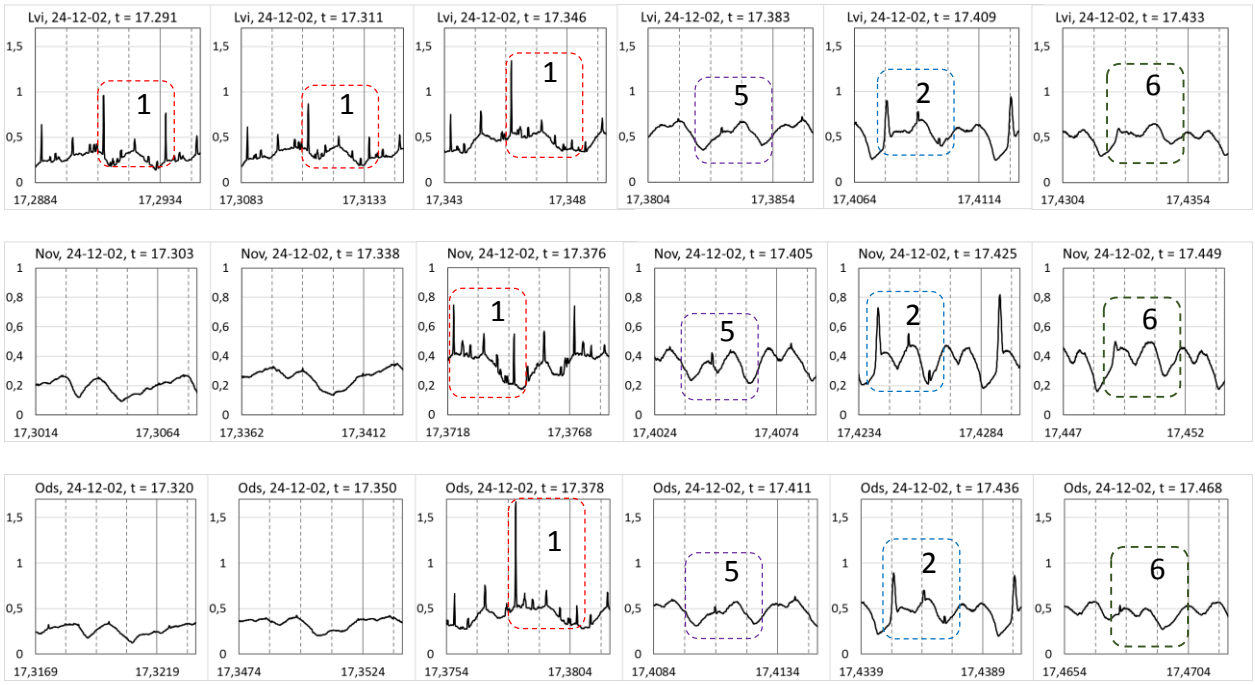

Figure 5a): Fragments of simulated light curves for northern OPs

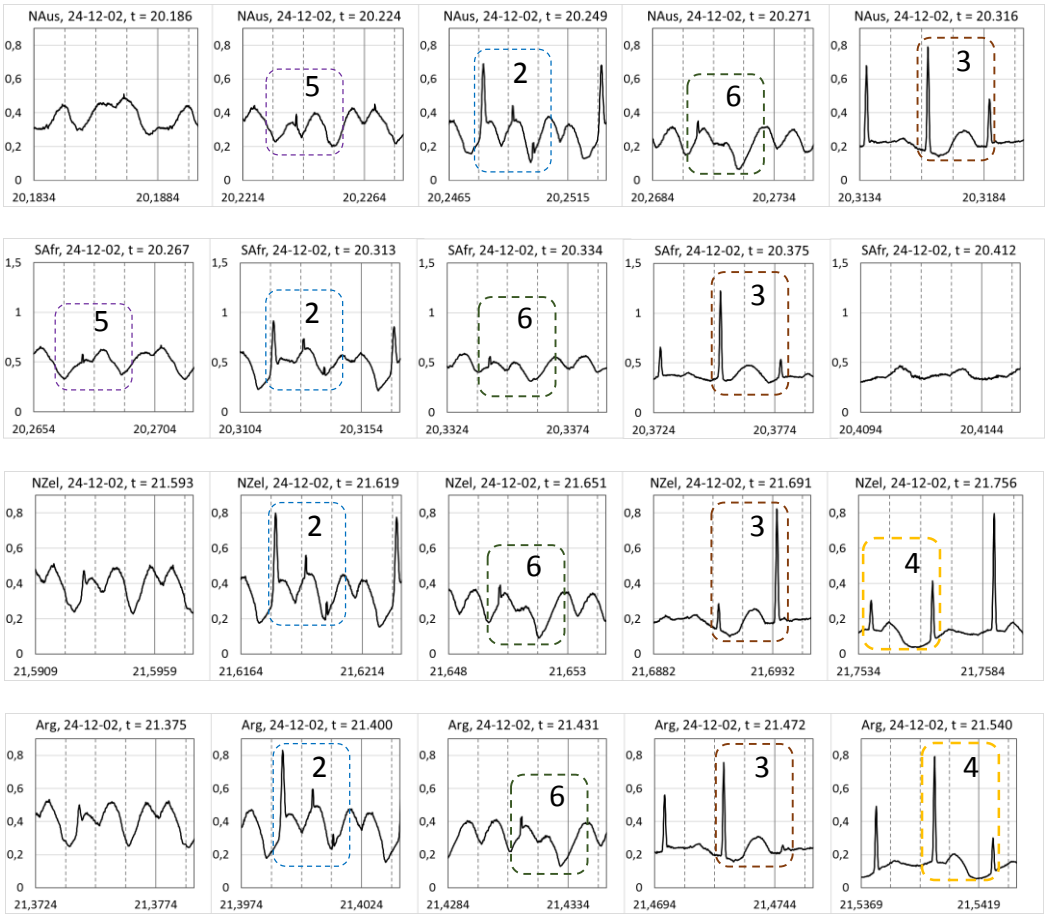

Figure 5b): Fragments of simulated light curves for southern OPs

Table 3: List of photometric patterns identified in different synthetic light curves and coordinates of the corresponding PAB vectors

No.	Date	Observ. Point	UT, h	RA of PAB	Decl. of PAB	Type of pattern	Phase angle	θ	Longitude of PAB	Latitude of PAB
1	02.12.2024	NAus	12.224	202.23	–21.67	5	86.9	44.6	214.50	18.00
2	02.12.2024	NAus	12.249	205.93	–5.75	2	89.7	56.4	202.00	29.80
3	02.12.2024	NAus	12.270	212.92	7.96	6	93.1	64.9	190.30	43.00
4	02.12.2024	NAus	12.316	238.91	26.95	3	100.0	70.4	163.90	70.50
5	03.12.2024	Arg	2.400	209.71	–11.47	2	78.3	56.2	209.00	30.50
6	03.12.2024	Arg	2.431	215.38	3.89	6	84.1	67.7	197.50	42.50
7	03.12.2024	Arg	2.472	237.50	25.44	3	97.7	73.5	168.00	69.50
8	03.12.2024	Arg	2.540	282.09	23.09	4	110.7	56.4	4.63	69.69
9	02.12.2024	NZel	10.619	208.66	–10.03	2	81.4	56.3	207.00	30.00
10	02.12.2024	NZel	10.650	213.39	4.52	6	88.1	65.5	194.50	41.60
11	02.12.2024	NZel	10.691	236.38	28.01	3	103.2	66.8	161.00	68.50
12	02.12.2024	NZel	10.759	282.28	25.49	4	114.6	50.9	12.00	69.80
13	02.12.2024	SAfr	19.267	210.71	–31.75	5	71.0	36.7	227.40	17.70
14	02.12.2024	SAfr	19.313	213.98	–15.42	2	67.9	56.3	216.50	30.50
15	02.12.2024	SAfr	19.334	218.41	–4.75	6	69.0	69.2	209.00	40.90
16	02.12.2024	SAfr	19.375	239.47	17.76	3	81.9	94.8	191.50	70.08
17	02.12.2024	Ods	15.378	214.83	–58.91	1	88.4	7.7	248.00	0.04
18	02.12.2024	Ods	15.411	208.44	–29.93	5	74.4	38.5	224.60	17.50
19	02.12.2024	Ods	15.437	212.56	–15.15	2	70.4	55.4	214.80	30.00
20	02.12.2024	Ods	15.468	217.31	–5.30	6	70.0	67.5	208.60	39.80
21	02.12.2024	Nov	15.377	197.52	–44.06	1	95.1	25.0	230.20	2.00
22	02.12.2024	Nov	15.405	203.56	–21.75	5	84.1	45.0	214.95	19.15
23	02.12.2024	Nov	15.425	208.32	–12.52	2	79.9	54.5	209.60	28.20
24	02.12.2024	Nov	15.449	213.14	–5.26	6	77.2	62.9	205.80	36.00
25	02.12.2024	Lviv	15.291	296.12	–61.76	1	102.0	28.0	286.20	0.50
26	02.12.2024	Lviv	15.311	281.93	–66.52	1	98.2	21.6	278.56	–1.04
27	02.12.2024	Lviv	15.346	232.18	–63.68	1	86.3	2.2	258.06	0.62
28	02.12.2024	Lviv	15.383	212.41	–33.33	5	68.3	34.8	229.64	17.70
29	02.12.2024	Lviv	15.409	214.44	–18.81	2	65.1	53.0	219.43	28.95
30	02.12.2024	Lviv	15.433	217.23	–10.29	6	65.4	64.0	213.76	36.51

4. Similar patterns selection

Structural analysis of the obtained light curves for seven OPs allows us to notice their sections similar to each other. The sections of the light curves in Fig. 5a) and 5b) bounded by dotted rectangles can be assigned to several different groups of patterns. The numbers of the group that include a given section are indicated in the corresponding rectangles. First of all, it is worth to select the sections containing series of short specular brightness flares, paying attention to the intervals between them. These relative intervals should be invariant with respect to changing observation conditions, including differences in the phase angle and orientation of the scattering plane (see Fig. 1 and Table 3). However, the amplitude of these flares can differ significantly due to possible differences in the degree of obscuration for the reflecting elements of the structure by other parts of the SO. Thus, we identified six different photometric patterns. At the same time, two of them (types 1 and 2) can be considered more reliable since they contain at least 3 specular flares. The third and fourth patterns contain two flares each, following after half a period, but considering the shape of the adjacent section of the light curves caused by diffuse scattering of light, these patterns can also be confidently considered similar to each other. Finally, the 5th and 6th patterns should be classified as mixed diffuse-specular, since they include only one mirror flare in their structure, and are therefore less reliable. Nevertheless, their shape and structure allow them to be unambiguously combined into two different groups.

Table 3 contains a list of patterns that we used to solve the problem of determining the orientation of the rotation pole using the method described above. For the average moment of each pattern given in the table, the equatorial coordinates of the PAB vectors corresponding to this moment are indicated. The values of the phase angle and the angle θ are also given there, as well as the spherical coordinates of the PAB in the coordinate system fixed with the rotation axis.

The equatorial coordinates of the PAB vectors corresponding to the moments of registration of a particular pattern are shown in Fig. 6a). We see that the points – traces of the PAB vectors form groups which ideally should have the form of arcs of small circles whose common center is the pole of the model's rotation axis (the pole specified in the calculations is indicated by a cross). Fig. 6b) shows the values of the spherical coordinates of the same PAB vectors in a coordinate system in which the z-axis coincides with the a priori specified axis of rotation. Here, the points corresponding to different patterns are located at different latitudes corresponding to the location of light-reflecting flat smooth faces and other surfaces forming this pattern on the surface of the spacecraft model. The numbers in the ovals in Fig. 6 indicate the identifiers of the patterns according to Table 3. The indicated points are located at the corresponding latitude with some scatter. The greatest spread is in the PAB latitude values related to the sixth, that is, mixed diffuse-specular type of pattern. As was said above, this scatter is caused by the non-synchronism of the change in the latitude of the PAB and the rotation of the SO during observations. It is the value of this scatter that determines error in estimating the coordinates of the rotation axis pole.

5. Results of calculating the direction of the rotation axis

Based only on the average moments of registration of the selected patterns and the corresponding equatorial coordinates of the PAB vectors in different passes of the simulated satellite (Table 3), we obtained a solution for the unknown coordinates of the rotation pole using the method described in (Koshkin et al., 2024). In this case, by changing the set of input data, it was possible to evaluate how this affects the resulting solution.

Using all 30 patterns from Table 3, the following solution for the pole was obtained: RA_pole = 262.04° and Decl_pole = 19.24°. For other combinations of input data, the solutions for the pole, residuals, and total deviation from true pole are given in Table 4.

As we expected, the best result (in terms of residuals with the true values of the rotation axis pole coordinates) was obtained using all four specular photometric patterns containing at least two specular brightness flares – the deviation from the given true pole is about 2.6 degrees. Also, a quite acceptable solution was obtained for all 30 selected patterns, the deviation was about 4.3 degrees. Using only the first type of pattern (five equatorial directions of the PAB vectors, most widely distributed in space) led to a solution that was accurate in the RA coordinate, but had an error of about 9 degrees in declination. The least accurate solution was obtained when only diffuse-specular patterns with one specular flare were used, the deviation was about 19 degrees. Apparently, this is due to increased errors in determining the average moments of these patterns and the corresponding PAB vectors due to the influence of differences in the observation geometry at different OPs.

Table 4: Coordinates of the model rotation pole obtained depending on the set of photometric patterns used

Patterns used	RA_pole, deg	Decl_pole, deg	(O-C)_RA, deg	(O-C)_Decl, deg	Deviation, deg
All patterns	262.0	19.2	2.0	–3.8	4.3
1-st patterns only	260.2	13.9	0.2	–9.1	9.1
1-4 patterns	262.4	24.1	2.4	1.1	2.6
5-6 patterns	249.0	7.2	–11.0	–15.8	19.2

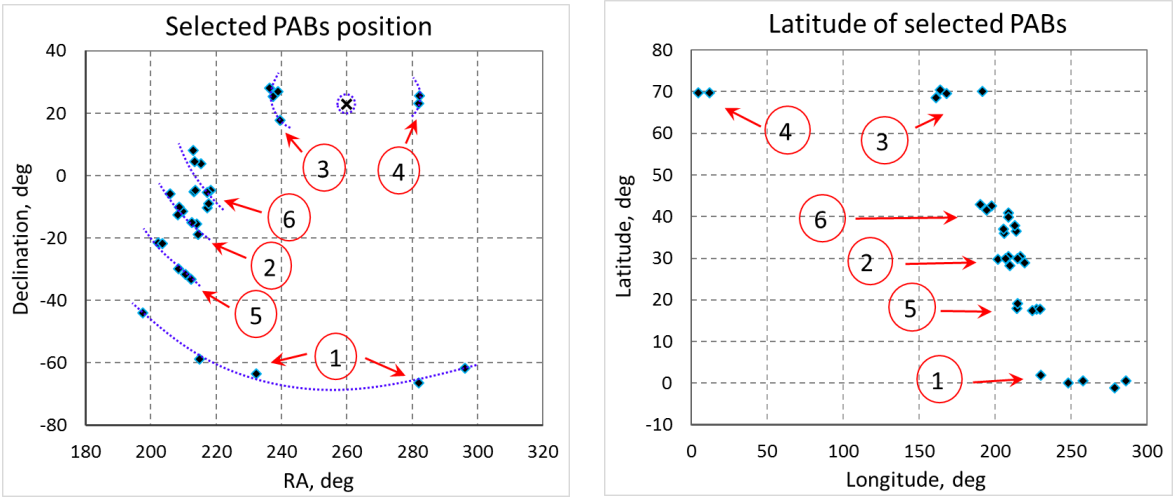

Figure 6: a) – Equatorial coordinates of the PAB vectors corresponding to the moments of pattern registration. The cross indicates the a priori given pole of the model's rotation axis. b) – Latitude and longitude of PAB vectors at the moments of observation of selected patterns. The numbers indicate the identifiers of the corresponding patterns.

Consider the diagram shown in Fig. 7, which relates two geometric parameters that influence the shape of the diffuse component of the light curves – the phase angle and the θ angle. Groups of similar patterns identified in different passages are also marked there.

We see that for the 5th diffuse-specular pattern in different passages the range of values of the angle θ was 10 degrees, and the range of values of the phase angle was 18.6 degrees. Despite this, the scatter of individual positions of the corresponding PAB vectors in Fig. 6a) and 6b) did not exceed 0.5 degrees, which means that the patterns were correctly identified on five different light curves. At the same time, for the patterns of the 6th type, the spread of positions of the PAB vectors in Fig. 6 is quite large, which is apparently due to the wide range of realized values of the phase angle: they are almost 28° (the values of the angle θ are limited to a range of only 6.3°). For the specular types of patterns, the values of the phase angle and the angle θ do not affect the presence of the flare on the light curves and, accordingly, the shape of the pattern. It is illustrated by a fairly wide range of realized values of these parameters, for example, for the 1st and 3rd patterns.

It is worth paying attention to the preserved sequence of the corresponding pattern appearance on the light curves in different passages. It is of course determined by the shape of the model body and the same direction of change in the PAB latitude in the overlapping ranges.

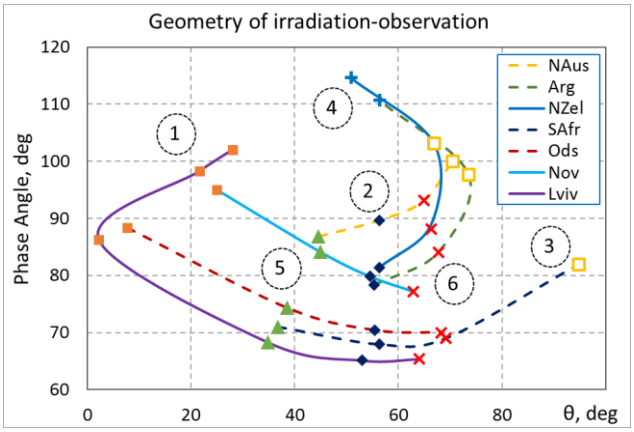

Figure 7: Geometrical conditions of illumination and visibility of the spacecraft model, realized in the described simulation experiment, in the form of trajectories in the parameter space "phase angle – angle θ" for the moments of appearance of patterns identified in different passes. Different types of patterns are depicted by different symbols, and their type (according to Table 3) is indicated by numbers in an oval.

6. Conclusions

The new method proposed in (Koshkin et al., 2024) for estimating the direction in space of the rotation axis of a complex-shaped SO rotating fairly quickly relative to the duration of passage over observation point requires verification on sets of photometric data of different types. In this paper, synthetic light curves of the SO model are used as input data for estimating the coordinates of the pole of the rotation axis. The light curves of the used model have a complex structure and contain, in addition to the diffuse component, also a significant number of short-term "specular" brightness flares. Over a time interval of about 14 hours, a set of seven simulated light curves was obtained for seven OPs located both in the northern hemisphere (within Ukraine) and in the southern hemisphere (widely distributed in longitude).

For all calculations of these synthetic light curves, it was assumed that the model rotates about one axis, fixed both in the body and unchanging in space. 30 short sections (less than the duration of one SO revolution) are identified on the light curves, and based on their similarity they are classified into six groups. For the average moments of their appearance on the light curves, the coordinates of the PAB were calculated and they were used to determine the direction (pole) of the model rotation axis. Comparison of the estimates of the rotation axis pole position obtained using different sets of photometric patterns with a given pole value used to calculate the light curves shows different values of the residuals for different sets of input data. The best result was obtained for photometric patterns containing at least two specular flares (types 1-4, 18 patterns in total) with a deviation from the true pole position of 2.6 degrees. The largest deviation from the true pole (about 19 degrees) was obtained for diffuse-specular patterns of types 5 and 6 (4 and 8 patterns, respectively).

Thus, this numerical experiment shows that diffuse-specular patterns similar in structure are successfully detected, which allows them to be used to determine the pole of rapidly rotating RSOs.

It should be emphasized once again that the change in the pattern of the light curves is determined by the ratio of the SO rotation speed and the rate of change of the PAB latitude in a given passage. The latter parameter is exactly the variable that determines which elements of the structure at a given moment reflect light specularly in the direction of the observer. However, the rotation of the object around its axis is an independent process and at the moments when the same values of the PAB latitude are reached, the same phases of the object rotation are not necessarily observed. This is the main fundamental reason for the errors in choosing the optimal moments of time and the corresponding PAB vectors, and, ultimately, in determining the orientation of the SO rotation axis by this method. Nevertheless, the considered method of photometric patterns can find wide application for various objects in orbit if there is a sufficient number of light curves for such an analysis, obtained in the tracking mode by a distributed network of observatories over a short period of time.

References

https://help.autodesk.com/view/3DSMAX/2023/ENU/
https://space.skyrocket.de/doc_sdat/dmsp-5d2.htm
Koshkin N.I., et al.: 2017, *OAP*, **30**, 226; 10.18524/1810-4215.2017.30.117655.
Koshkin N. (ed.), et al.: 2021, ATLAS of light curves of space objects Odessa I.I. Mechnikov national univ., Ukraine research inst. "Astronomical observatory", Dep. of space research. – Odesa, 2021. – Part 6 (2019 – 2020). – 200 p.; 10.18524/Atl_v.6(2019-2020).2021
Koshkin, N.I., Melikyants S., et al.: 2019, *OAP*, **32**, 158; 10.18524/1810-4215.2019.32.183899.
Koshkin N., Shakun L., et al.: 2018, *OAP*, **31**, 179; 10.18524/1810-4215.2018.31.147807.
Koshkin N., Shakun L., et al.: 2024, *AdSpR*, **74**, 11, 5725; 10.1016/j.asr.2024.08.038.
Kudak V., et al.: 2024, *ArtSat*, **59**, Iss. 2, 42; 10.2478/arsa-2024-0003.